Optimization of Alkali Treatment of Rice Husk Ash for Producing an Alternative Alkali Activator *via* Response Surface Methodology

Herry Prabowo [a,b,*] Idawati binti Ismail [a,*] Md Rezaur Rahman [a,*] Azizah binti Abdul Nassir [a] Mohammad Abdul Mannan [c] Maha G. Batterjee [d] K. S. Alblawi [e] Jehan Y. Al-Humaidi [f] and Mohammed Muzibur Rahman [g]

*Corresponding author: iidawati@unimas.my; rmrezaur@unimas.my; herryprabowo@polnep.ac.id

DOI: 10.15376/biores.21.3.7516-7540

GRAPHICAL ABSTRACT

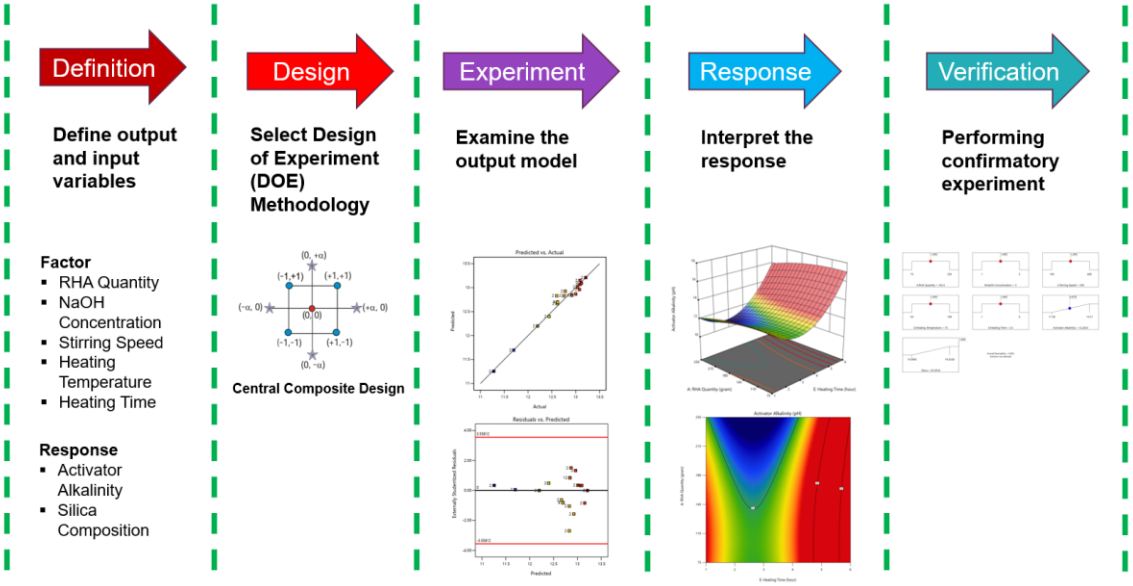

Optimization of Alkali Treatment of Rice Husk Ash for Producing an Alternative Alkali Activator *via* Response Surface Methodology

Herry Prabowo [a,b,*] Idawati binti Ismail [a,*] Md Rezaur Rahman [a,*] Azizah binti Abdul Nassir [a] Mohammad Abdul Mannan [c] Maha G. Batterjee [d] K. S. Alblawi [e] Jehan Y. Al-Humaidi [f] and Mohammed Muzibur Rahman [g]

The geopolymer field is flourishing, as researchers work to lessen the reliance on conventional cements as building materials. However, high price and energy-intensity of commercial alkaline activators hamper the usage of geopolymers. Bio-based waste materials are efficacious in mitigating the environmental concerns for alkaline activators, but the synthesis process of this alternative alkali activator requires further research, especially on the optimization for RHA dissolution parameters. The objective of this study was to optimize the alkali treatment process on rice husk ash (RHA) using response surface methodology. The effect of five factors, *i.e.*, RHA quantity, sodium hydroxide concentration, stirring speed, heating temperature, and heating time on two output responses, *i.e.,* activator alkalinity and silica composition of alternative activators, were investigated. Central composite design provided the combination for an optimum alternative activator, which was 162.5 g of RHA quantity, 3M of NaOH concentration, 350 RPM of stirring speed, 75 °C of heating temperature, and 3.5 h of heating time with $R^2 > 0.91$ of reduced quadratic models. The activator alkalinity (pH) and silica composition (wt%) for alkali treatment processed activator were 12.1 and 20.3 respectively.

DOI: 10.15376/biores.21.3.7516-7540

Keywords: Alkali treatment; Alternative activator; Rice husk ash; Response surface methodology

Contact information: a: Department of Civil Engineering, Faculty of Engineering, Universiti Malaysia Sarawak, 94300 Kota Samarahan, Sarawak, Malaysia; b: Department of Architectural Engineering, Politeknik Negeri Pontianak, Jl. Jenderal Ahmad Yani, Kota Pontianak, Kalimantan Barat 78124, Indonesia; c: School of Civil Engineering, Faculty of Engineering, Papua New Guinea University of Technology, LAE411, Morobe Province, Papua New Guinea; d: Department of Chemistry, College of Sciences & Arts, King Abdulaziz University, Rabigh, Saudi Arabia; e: Chemistry Department, Faculty of Science, King Abdulaziz University, Jeddah 21589, Saudi Arabia; f: Department of Chemistry, College of Science, Princess Nourah bint Abdulrahman University, P.O. BOX 84428, Riyadh 11671, Saudi Arabia; g: Center of Excellence for Advanced Materials Research & Chemistry Department, Faculty of Science, King Abdulaziz University, Jeddah 21589, Saudi Arabia;

** Corresponding author: iidawati@unimas.my; rmrezaur@unimas.my; herryprabowo@polnep.ac.id*

INTRODUCTION

Geopolymer concrete has emerged as a promising alternative construction material compared to Ordinary Portland Cement (OPC) (Farooq *et al.* 2026). The manufacturing process of OPC is known to have significant ecological consequences, primarily due to the substantial emission of greenhouse gases (GHG) (Neupane 2022). On the contrary,

geopolymers are estimated to reduce global warming potential by 7% to 50% compared to OPC (Cong *et al.* 2024). Despite geopolymers having a lower GHG output, their utilization still leads to environmental issues due to chemical alkali activators. Alkali activator is one of the main constituent materials of geopolymer that are costly and energy demanding (Ricciotti *et al.* 2025).

Researchers have studied the feasibility of employing silica-rich resources from agricultural waste to synthesize alternative alkali activators. Rice husk is one of the popular agro-wastes that contribute significantly to global waste generation (150 million tons annually) (Kordi *et al.* 2024). Traditionally, rice husk was disposed of through practices such as burning, resulting rice husk ash (RHA) (Al-Alwan *et al.* 2024). This RHA is particularly useful because they contain soluble silicates and alkali metal ions, which are essential for the polymerization process in geopolymer concrete (Barragán-Ramírez *et al.* 2024). Previous studies showed that the synthesis of alternative sodium silicates from these resources is viable and yields an activator comparable to commercial ones (Alnahhal *et al.* 2021). Despite the promising potential to develop waste-derived alkaline activators, the properties of activators synthesized from RHA have not been fully understood in terms of the effects of the extraction process on the alkalinity and silica composition.

Various studies have shown promising results on silicate extraction from RHA (Rajan and Kathirvel 2021; Nzereogu *et al.* 2023; Trevizan Pelissaro *et al.* 2023). The dissolution of RHA in NaOH solution, which is an alkali treatment process, is a well-known extraction technique. The suspensions of RHA and NaOH were exposed to heating and stirring to induce the dissolution of silica from RHA into the NaOH solution. Parameters influencing the efficiency of this alkali treatment process have been investigated. However, the optimization for RHA dissolution (*i.e.*, process temperature and duration, NaOH solution concentration, RHA quantity, and stirring speed) have not yet been confirmed.

Response surface methodology (RSM) is widely used to provide optimized condition by analyzing the effects of different independent variables (Veza *et al.* 2023). Many authors have claimed the suitability of using central composite design (CCD) of RSM (RSM-CCD) to optimize the independent variables in their research article (Pattanayak *et al.* 2024; Yao *et al.* 2024; Maaze *et al.* 2025). RSM-CCD is the choice to optimize the process parameters in this study as well as replace the conventional time-consuming methods. It efficiently models complex, non-linear relationships with a reduced number of experimental runs compared to a full factorial design. When dealing with 5 factors, CCD provides a robust, sequential, and rotatable framework that helps find the optimal point for production (Ghelich *et al.* 2019; Alawadhi *et al.* 2021).

The synthesis of alternative alkali activators has been the subject of extensive study. Despite this, there are very few studies on the optimization of alternative alkali activator parameters using RSM (Girish *et al.* 2026) based on the principles of design of experiments (DoE). Furthermore, the present research investigates simultaneously 5 parameters of alkali treatment, *i.e.*, RHA quantity, NaOH concentration, stirring speed, heating temperature, and heating time. Among those independent variables, stirring speed is rarely investigated. The aim was to determine the optimum values of those 5 factors for alternative activators with maximum alkalinity and silica composition. Maximum alkalinity provides the necessary hydroxide ions (OH^-) required to efficiently break down the siloxane bonds (Si-O-Si) (Wan *et al.* 2025). Meanwhile, high silica composition is crucial for providing the active silicate species needed to form the rigid geopolymer binding gel (Gao *et al.* 2022; Bezerra *et al.* 2023) during subsequent concrete applications.

The findings contribute to the development of sustainable alternatives that potentially lower the overall environmental impact.

EXPERIMENTAL

Materials

Rice husk was collected from Parit Gadoh, a rice mill located at Kubu Raya, West Kalimantan, Indonesia. The as-received rice husk was burnt in a drum kiln without any pre-treatment. It was burnt at 500 °C for 12 h (Nair *et al.* 2008; Albert Daud *et al.* 2020) to become rice husk ash (RHA). Burning duration and temperatures are intended for maximizing the amorphous content of the RHA, as higher temperature and shorter times would induce the formation of crystalline SiO_2 (Hamidu *et al.* 2025). After burning, the RHA was placed in stainless steel tray and cooled down at ambient temperature for 24 h. Then, the RHA was sieved to pass through a 0.3 mm sieve. Next, the RHA was ground to achieve a mean particle size (d_{50}) of 31.38 µm, as per literature suggestions (Kamseu *et al.* 2017; Kim *et al.* 2025).

This study used RHA as a silica source to produce geopolymer's alternative alkali activator (AA) solutions *via* alkali treatment. Laboratory grade sodium hydroxide (NaOH) pellets (98.0 % purity, Sigma-Aldrich, Germany) were used to prepare the solution for AA synthesis. The NaOH solutions based on various molarity were prepared with distilled water.

Response Surface Methodology (RSM)

RSM is an optimization tool based on statistical and mathematical techniques for optimizing processes and simultaneously establishing a relationship between the factors and responses. The Stat-Ease 360 version 25.0.6 (Stat-Ease, Inc., Minneapolis, MN) was used to design the experiment, examine and interpret the output model, and perform verification. Optimization for maximum alternative AA alkalinity and silica composition was employed using a CCD model. CCD was selected because it is highly efficient for fitting second-order surface models, allowing for the comprehensive evaluation of quadratic and interaction effects among multiple variables with a reduced number of experimental runs (Ghelich *et al.* 2019). Five numeric factors are included in the design: RHA quantity (A) in gram, NaOH concentration (B) in M, stirring speed (C) in rotation per minute (RPM), heating temperature (D) in °C, and heating time (E) in hour. The design generated a total of 50 experimental runs, including 32 factorial points (–1, +1), 10 axial points (–α, +α), and 8 center points (0) to properly evaluate pure experimental error. The independent variables were evaluated at five coded levels (–α, –1, 0, +1, +α), and all runs were fully randomized. The CCD model of factors in the form of coded and actual values is listed in Table 1.

The design was represented by a second-order polynomial regression model, as follows:

$$Y = \beta_0 + \sum_{i=1}^{k} \beta_i X_i + \sum_{i=0}^{k} \beta_{ii} X_i^2 + \sum_{1 \le i \le j}^{k} \beta_{ij} X_i X_j + \varepsilon \quad (1)$$

where Y represents the responses (activator alkalinity and silica composition). The factors X_i, β_0, β_i, β_{ii}, β_{ij}, and ε in Eq. 1 are the process factors, offset coefficient, linear coefficients, quadratic coefficients, interaction coefficients, and residuals associated with the experiments, respectively.

Analyses include factors significantly affecting the responses using the analysis of variance (ANOVA) and coefficient of determination (R^2), 3D RSM plots, and contour plots based on the interactions between parameters. The ANOVA results show P-values and model F-values. The P-values less than 0.05 indicate model terms are significant, and the higher F-values implied model significance and less chance that the values could be due to noise.

Most importantly, the software suggests optimum factor conditions for specific product yields, reflecting the sensitivity of the variable factors. The R^2 values (close to 1), adjusted R^2, and predicted R^2 values were analyzed to optimize process parameters. The difference between predicted and adjusted R^2 is supposed to be less than 0.2 in well-fit models. Also, a good precision value higher than 4 reflects a desirable signal-to-noise ratio. The diagnostic tools present in the software helped ensure the model helps predict the target responses.

Table 2 lists the values of the studied factors and results from the experiment. The five factors, RHA quantity, NaOH concentration, stirring speed, heating temperature, and heating time have lower and higher value inputs ranging from 75 to 250 g, 0.5 to 5 M, 100 to 600 RPM, 50 to 90 °C, and 1 to 5 h, respectively. During ANOVA model analysis, the values in Table 2 were adjusted to accommodate the reduction of insignificant terms and noise in the model. It was described in the effect of variables subsection. RHA quantity ranges were selected to establish a solid-to-liquid ratio around 0.5 to 0.2 that provides sufficient silica (Luukkonen *et al.* 2018; Font *et al.* 2020; Alnahhal *et al.* 2024). The NaOH concentrations were fixed based on the necessary alkalinity to break down siloxane bonds efficiently (He *et al.* 2013; Tong *et al.* 2018). Meanwhile, heating temperature and heating time inputs were obtained from previous studies which indicated that elevated heat and extended durations enhance dissolution up to a specific threshold (Tong *et al.* 2018; Font *et al.* 2020; Kallamalayil Nassar and Kathirvel 2023; Alnahhal *et al.* 2024). The stirring speed range was specifically selected to ensure adequate suspension of RHA particles.

Table 1. Variables and Coded Levels

Variables	Units	Symbol	Coded Level					References
			-α	-1	0	+1	+α	
Factor								
RHA Quantity	g	A	75	100	125	175	250	(Luukkonen *et al.* 2018; Font *et al.* 2020; *Alnahhal et al.* 2024)
NaOH Concentration	M	B	0.5	2	3	3.5	4	(He *et al.* 2013; Tong *et al.* 2018)
Stirring Speed	RPM	C	100	200	400	500	600	NA
Heating Temperature	°C	D	50	60	70	80	90	(Tong *et al.* 2018; Font *et al.* 2020; Kallamalayil Nassar and Kathirvel 2023)
Heating Time	h	E	1	2	3	4	5	(Tong *et al.* 2018; Alnahhal *et al.* 2024)
Response								
Activator Alkalinity	pH	R1						
Silica Composition	wt%	R2						

Synthesis of Alternative Activator

An alkali treatment process was used to synthesize alternative AA by dissolving rice husk ash (RHA) powder in a NaOH solution under continuous magnetic stirring while maintaining heat. The alkali treatment was processed using magnetic stirring hot plate Corning PC-620D, NY, USA. This process was commonly used by previous researchers to produce alternative alkali activator solutions (Tchakouté *et al.* 2016; Alnahhal *et al.* 2024).

The NaOH pellets at first were mixed with 500 mL distilled water in a glass beaker and then cooled to ambient temperature. RHA was then added to the sodium hydroxide solution in a 1000 mL glass beaker, which was placed on a hot plate magnetic stirrer. The solid to liquid ratio ranged from 0.5 to 0.2. The alkali treatment was initiated, which involves continuous stirring of the prepared mixture at a previously mentioned temperature and duration ranges with the aid of a hot plate magnetic stirrer. During the treatment, the beaker was covered with a laboratory film to minimize evaporative losses. The temperature of the mixture was monitored using a thermometer submerged directly in the suspension, and was maintained at the target value with a tolerance of ± 2 °C.

The next step was the filtration process after allowing the mixture to cool to room temperature. The filtration was performed under atmospheric pressure using Whatman No. 42 filter paper (pore size 2.5 μm) to separate solid particles from liquid solutions. The primary objective of the filtration was to remove any undissolved particles that might have remained in the solution after synthesis. Once the filtration process was completed, the resulting solution was carefully transferred into bottles, and the final volume of the recovered filtrate was recorded for subsequent analyses.

Table 2. Design of Experiment and Results of the Central Composite Design

Std	Run	Factor					Response	
		A	B	C	D	E	R1	R2
36	1	250	3	400	80	4	11.70	17.3419
3	2	125	3	400	80	4	12.75	17.4296
47	3	100	3	400	80	4	13.00	17.4073
19	4	75	3	400	80	4	12.92	16.0366
49	5	75	0.5	400	80	4	11.28	17.0571
29	6	75	3.5	400	80	4	12.62	15.5593
13	7	75	2	400	80	4	12.61	16.3228
35	8	75	2.5	400	80	4	12.60	17.3388
6	9	75	3	400	80	4	12.92	16.0366
16	10	75	3.5	400	80	4	12.62	15.5593
46	11	75	4	400	80	4	12.44	15.0905
22	12	75	3.5	400	80	4	12.62	15.5593
5	13	75	3	100	80	4	13.09	17.1806
31	14	75	3	200	80	4	13.08	16.2293
1	15	75	3	400	80	4	12.92	16.0366
30	16	75	3	600	80	4	13.09	15.6729
42	17	75	3	400	50	4	13.12	19.2615
25	18	75	3	400	60	4	13.04	19.3328
4	19	75	3	400	70	4	12.78	16.7563
32	20	75	3	400	80	4	12.92	16.0366
40	21	75	3.5	400	80	4	12.62	15.5593
23	22	75	3	400	80	1	13.21	15.3833
28	23	75	3	400	80	2	12.20	18.1695

34	24	75	3	400	80	4	12.92	16.0366
9	25	75	3	400	80	4	12.92	16.0366
7	26	75	3	400	80	4	12.92	16.0366
18	27	250	3	400	80	4	11.70	17.3419
24	28	125	3	400	80	4	12.75	17.4296
45	29	100	3	400	80	4	13.00	17.4073
15	30	75	3	400	80	4	12.92	16.0366
50	31	75	0.5	400	80	4	11.28	17.0571
39	32	75	3.5	400	80	4	12.62	15.5593
8	33	75	2	400	80	4	12.61	16.3228
48	34	75	2.5	400	80	4	12.60	17.3388
10	35	75	3	400	80	4	12.92	16.0366
12	36	75	3.5	400	80	4	12.62	15.5593
41	37	75	4	400	80	4	12.44	15.0905
26	38	75	3.5	400	80	4	12.62	15.5593
43	39	75	3	100	80	4	13.09	17.1806
37	40	75	3	200	80	4	13.08	16.2293
33	41	75	3	400	80	4	12.92	16.0366
38	42	75	3	600	80	4	13.09	15.6729
20	43	75	3	400	50	4	13.12	19.2615
2	44	75	3	400	60	4	13.04	19.3328
27	45	75	3	400	70	4	12.78	16.7563
44	46	75	3	400	80	4	12.92	16.0366
11	47	75	3.5	400	80	4	12.62	15.5593
17	48	75	3	400	80	1	13.21	15.3833
14	49	75	3	400	80	2	12.20	18.1695
21	50	75	3	400	80	4	12.92	16.0366

Test Methods to Characterize Materials

Particle size analyzer

Particle size distribution (PSD) of ground RHA was determined with a laser diffraction particle size analyzer using CILAS 1090 equipment (Ariane group, France). The PSD was measured by using RHA suspension in water and detecting particle sizes by the laser-beam reflection, recalculating the distribution of the particles through Fourier transform methods. The RHA suspension in water was prepared to obtain obscuration around 15% and ultrasonicated for 5 minutes prior to measurement to prevent particle agglomeration.

Scanning electron microscopy

This study used scanning electron microscopic (SEM) analysis to investigate the particle shape and surface texture of RHA. SEM characterization was carried out using the SEM Hitachi TM4000 model, Japan. SEM was operating at an accelerating voltage of 15 kV. Prior to imaging, the RHA samples were sputter-coated with a thin layer of gold to enhance electrical conductivity and prevent charge accumulation.

Energy dispersive X-ray spectroscopy

The elemental composition of RHA was examined using the energy dispersive X-ray spectroscopy (EDX). EDX characterization was carried out using the Bruker EDX (Bruker, Germany) with ESPRIT software. To determine the silica composition (wt%) of the alternative activator, 5 mL of the synthesized solution was dried in an open container in a closed drying oven at 60 °C for 7 d. Instead of prolonged ambient drying, a fixed drying protocol was applied by storing the samples in a desiccator for 14 d to ensure

consistent moisture removal. EDX was selected for this purpose because it provides a reliable semi-quantitative elemental profile of the dried solid residue. The reported silica composition for each run represents the average of three replicate EDX spot analyses.

pH Measurement

The alkalinity of the synthesized alternative alkali activator was quantified by pH measurement. The pH was determined with a Benchtop Fisher Scientific Accumet AB150 pH meter. Prior to use, the pH meter was calibrated using standard buffer solutions at pH 4.01, 7.00, and 10.01. All measurements were conducted at a controlled room temperature of 25 ± 1 °C, and the reported alkalinity for each experimental run was based on the average of three replicate measurements to ensure accuracy.

RESULTS AND DISCUSSION

Characterization of Materials

Particle size analyzer

The particle size *vs*. cumulative passing graph is shown in Fig. 1. The cumulative passing curve showed a median particle diameter (D_{50}) of 31.4 μm. Meanwhile, D_{10} and D_{90} were obtained as 5.97 μm and 63.3 μm respectively. Literature suggested RHA was milled to attain average particle size in the range 5 to 40 μm before it was dissolved in an NaOH solution (Adesanya *et al.* 2021). This approach is based on the rationale that particle size reduction increases the available specific surface area, thereby facilitating dissolution and improving reaction kinetics with NaOH.

Finer RHA particles have a higher specific surface area, which is crucial for enhancing the reactivity of the silica content. This is because a larger surface area allows for more interaction sites between the silica and the NaOH solution (Zulfiqar *et al.* 2015). Moreover, the reactivity of the amorphous silica in RHA is directly proportional to its specific surface area (Endale *et al.* 2023; Hamidu *et al.* 2025).

Scanning electron microscopy

SEM images, as shown in Fig. 2., revealed that RHA consisted of irregular and angular shaped particles. This morphology is frequently observed in amorphous silica found in RHA aligns with previous studies. Meanwhile, SEM alone cannot definitively confirm the non-crystalline nature of the silica content (Sompech *et al.* 2016; Sarma *et al.* 2024).

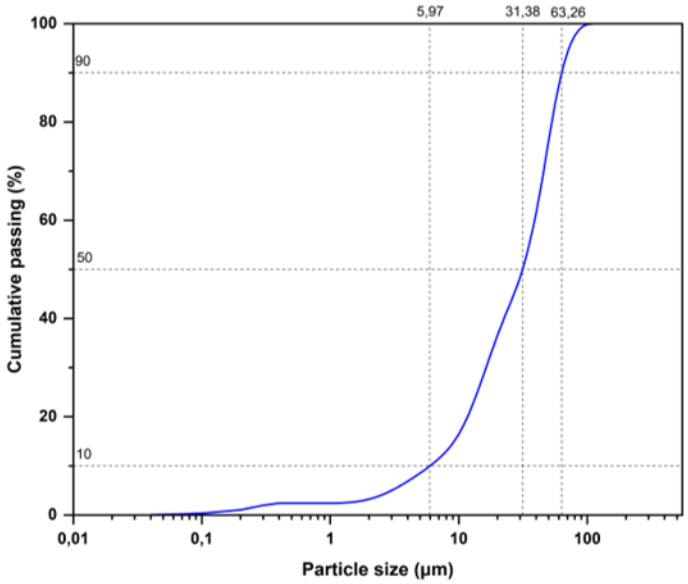

Fig. 1. Rice husk ash particle size distribution

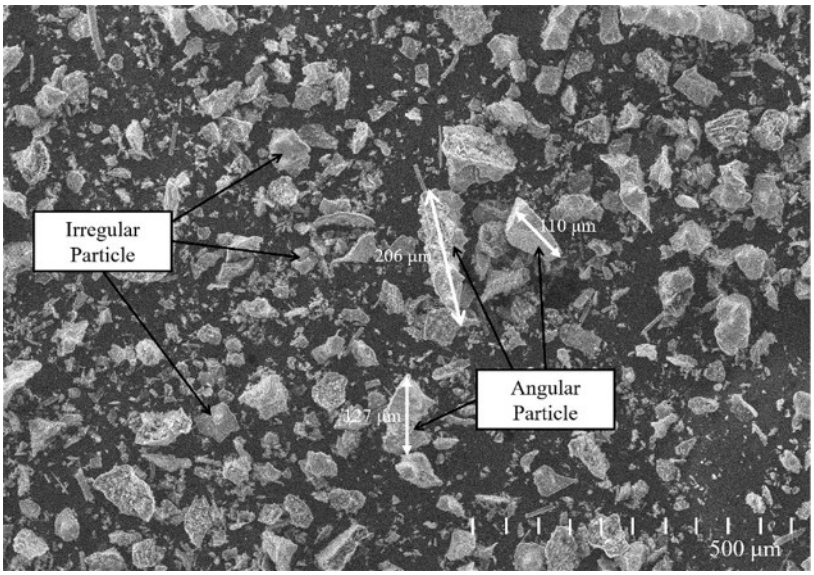

Fig. 2. SEM of rice husk ash

Energy dispersive X-ray spectroscopy

Figure 3 presents the energy dispersive X-ray (EDX) spectrum and the corresponding elemental composition of the synthesized RHA. The spectrum reveals a distinct elemental profile characterized by sharp characteristic peaks for Silicon (Si) and Oxygen (O), alongside a significant peak for Carbon (C). These peaks indicate the elemental presence of silicon and oxygen, which is consistent with silica as the primary inorganic constituent, coexisting with carbon. However, EDX alone cannot definitively confirm exact chemical phases such as SiO_2 or establish the presence of a residual organic carbon matrix with certainty.

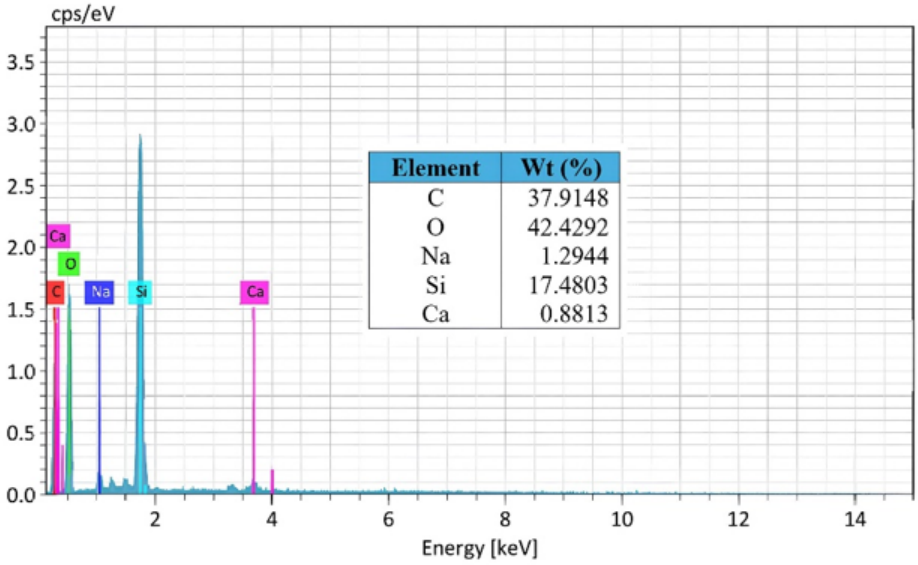

Fig. 3. EDX of rice husk ash

Effect of Variables on Alternative Alkaline Activator Alkalinity

Mathematical model for predicting alkalinity of alternative activator

RSM was used to develop mathematical models from the experimental results and predicted responses, where the output is influenced by several variables. This mathematical model is derived from the relationship between the input and output parameters. The factors RHA quantity, NaOH concentration, stirring speed, heating temperature, and heating time are represented as A, B, C, D and E, respectively (Table 1).

The investigated factors and their corresponding experimental results are presented in Table 2. Initially, the experimental matrix was generated using a Central Composite Design (CCD), comprising 50 randomized runs: 32 factorial points, 10 axial points, and 8 center points. Upon recording the measured responses for each run, a full quadratic regression model and Analysis of Variance (ANOVA) were formulated using the Stat-Ease software. Because the initial full model contained statistically insignificant terms that adversely affected the fit statistics, a term-reduction procedure utilizing backward elimination was applied to improve the Predicted R^2, Adjusted R^2, and Adequate Precision values. Furthermore, repeated identical response values were incorporated to enhance the model's predictive power and interpretability. Later, the predictive accuracy and reliability of the reduced model were verified by conducting confirmatory experimental runs.

The activator pH ranged from 11.3 to 13.2. The highest pH value was 13.2 at of 75 g RHA, 3M NaOH concentration, 400 RPM stirring speed, 80 °C heating temperature, and 1.0 h heating time. Meanwhile, the lowest pH was 11.3 at 75 g RHA, 0.5M NaOH concentration, 400 RPM stirring speed, 80 °C heating temperature, and 4-h heating time.

The best-fitting model was found to be a reduced quadratic model. A term-reduction procedure was performed using backward elimination to remove statistically insignificant interaction terms ($P > 0.05$) from the full model. These interaction terms were excluded from the final reduced model to simplify the equation and improve its predictive capability without modeling noise. Equation 2 represents the mathematical model (in terms of actual factors) for predicting alternative activator alkalinity:

$$R1 = +13.5499 + 0.0099A + 1.7085B - 0.0032C - 0.0084D - 1.9180E - 5.0653e\text{-}05A^2 - 0.3071B^2 + 4.3466e\text{-}06C^2 + 0.4434E^2 \quad (2)$$

The + sign in the equation denotes the synergistic effects of variables, and the antagonistic effects are indicated by the − sign in the equation (Niu *et al.* 2022). While the stirring speed (C), heating temperature (D), and heating time (E) had adverse effects on the activator alkalinity, the RHA quantity (A) and NaOH concentration (B) had a positive effect on the yield. Furthermore, the second-order term A^2 and B^2 posed unfavorable effects, while C^2 and E^2 were favorable.

ANOVA for the prediction quadratic model

Table 3 shows ANOVA results based on the RSM study produced by Stat-Ease 360 version 25.0.6. The P-value for the quadratic model of alternative activator alkalinity was significant ($P < 0.0001$), which shows that the results were significant, and the model was excellent for predicting the response (alternative activator pH). Furthermore, the model F-value of 109.6003 implies the model was significant, since there was only a 0.01% chance that an F-value this large could occur due to noise. In this case, A, B, D, E, A^2, B^2, C^2, and E^2 were significant model terms (note: A is RHA quantity; B is NaOH concentration; C is stirring speed; D is heating temperature; E is heating time). Therefore, the hypothesis of this study—the significant effect of factors—was confirmed. Values greater than 0.1000 indicate that certain of the model terms were not significant. The insignificant term, C, had a P-value of 0.3213. Statistical insignificance indicates that the study lacked sufficient evidence to prove that the variable being tested had any effect. Most importantly, the stirring speed (C) did not have significance in the model. In this model, the Stat-Ease software did not show the lack of fit value after backward elimination was used. It reduced the number of model terms, which changed the sum of squares. Although without lack of fit statistics, the model still can be evaluated by utilizing several parameters such as R^2, Adjusted R^2, Predicted R^2, and Adequate Precision. Moreover, predicted *vs.* actual plot and residual *vs.* predicted plot also can be used to validate the model (Chen and Chen 2025).

Table 3. ANOVA for Quadratic Model of Activator Alkalinity

Source	Sum of Squares	Degree of Freedom (df)	Mean Square	F-value	*P*-value	Significance
Model	9.1453	9	1.0161	109.6003	< 0.0001	significant
A-RHA Quantity	2.4063	1	2.4063	259.5404	< 0.0001	
B-NaOH Concentration	0.1216	1	0.1216	13.1120	0.0008	
C-Stirring Speed	0.0094	1	0.0094	1.0085	0.3213	
D-Heating Temperature	0.1611	1	0.1611	17.3789	0.0002	
E-Heating Time	1.0128	1	1.0127	109.2361	< 0.0001	
A^2	0.2268	1	0.2268	24.3123	< 0.0001	
B^2	2.3916	1	2.3916	257.9559	< 0.0001	
C^2	0.2222	1	0.2222	23.9679	< 0.0001	
E^2	1.0813	1	1.0813	116.6229	< 0.0001	

Std. Dev.	0.0963		R^2	0.9610		
Mean	12.7196		Adjusted R^2	0.9523		
CV %	0.7570		Predicted R^2	0.9497		
PRESS	0.4785		Adequate Precision	45.3787		

The R^2 of 0.9610 achieved is indicative that the model produced was valid and closely fitted to the experimental data. This result was similar to one reported by Adamu *et al.* (2019). The predicted R^2 of 0.9497 was in reasonable agreement with the adjusted R^2 of 0.9523. The difference between predicted R^2 and adjusted R^2 was found to be 0.0026, which is within the required limit (not more than 0.2) for a good model. R^2 can improve by addition of more independent variables therefore goodness of fit cannot be concluded from value of R^2 alone. Conversely adjusted R^2 only increases with variables that have strong correlation with the dependent variable otherwise it decreases. On the other hand, predicted R^2 is an indication of how well the model developed produces responses for new observation and whether the model is complicated or not. Therefore, adjusted R^2 and predicted R^2 are more desirable properties for goodness of fit in statistics. In this model, R^2 was close to 1; thus, the data and the models produced were very significant.

The mean pH value of alternative activators was 12.7. The standard deviation in activator alkalinity was ± 0.0963, which is acceptable, while the coefficient of variation (CV %) in activator alkalinity was 0.757%, which is below the acceptable level of 10%, reflecting a good model. In addition, the signal-to-noise ratio (S/N ratio) was measured by adequate precision (AP). Therefore, when the AP value is greater than 4, the model discrimination is considered satisfactory (Rocha *et al.* 2023). Moreover, the predicted values' ranges at the design point to the average prediction error are compared using AP (Khalid *et al.* 2024). Therefore, the AP obtained from the experimental values (45.3787) could be considered adequate, which is a good sign and implies that the model can be used to navigate the design space (Alkharisi and Dahish 2025). The descriptive statistics of the model, factors' sum of the squares, and mean square values are shown in Table 3.

Diagnostics of actual versus predicted responses

Considering the positive note of the prediction model from the statistics, the Stat-Ease Software gives other diagnostic tools based on the experimental data and model for further analysis. The predicted *versus* actual plot and residual *versus* predicted are discussed here. These plots help to understand if there are any outliers in the experimental results (Fig. 4). Figure 4a shows a predicted plot of the actual responses which is roughly a straight line, which shows the model's good quality in predicting the responses with R^2 value of 0.9610. The correlation between the predicted and actual activator alkalinity, and the linearity shows the model is useful for predicting the alkalinity efficiently. Meanwhile, the residual *versus* predicted plots, depicted in Fig. 4b, shows constant variants with no specific trends and no outliers (no points above the red line).

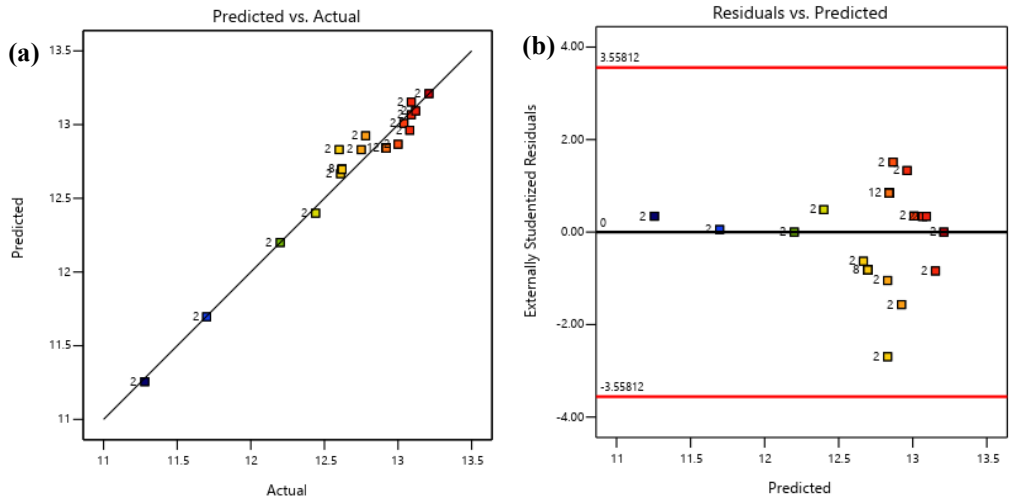

Fig. 4. a: Predicted *vs*. actual plot; and b: Residuals *vs*. predicted

Analysis of response surface plots of alternative activator alkalinity

Figure 5 represents the three-dimensional plots of the interaction between the dependent variables and independent variables for alternative activator alkalinity. Figures 5a and 5b show that the alkalinity of alternative activators tended to reach optimum as the RHA quantity and NaOH concentration was increased. After reaching optimum peak, the alkalinity decreased with increasing RHA quantity and NaOH concentration. Initially, increasing the RHA quantity provides more amorphous silica available to be dissolved by NaOH. This increases the silicate content in the solution, which is crucial for forming the geopolymer binding gel. The dissolution process is limited by the amount of NaOH available. Once the RHA quantity exceeds the capacity of the NaOH to dissolve it, saturation, the dissolution efficiency drops. The excess RHA remains as undissolved solid residue, *e.g.*, unreacted particles rather than contributing to the active silicate species (Muñoz-Castillo *et al.* 2025).

Figures 5c and 5d show that the alkalinity was almost constant when the stirring speed increased. On the other hand, alkalinity decreased with the increase of RHA quantity. Stirring speed primarily influences the mass transfer rate rather than the chemical equilibrium itself. While adequate stirring is necessary to keep the RHA particles suspended and ensure contact with the NaOH solution, increasing the speed beyond a certain point does not significantly change the final extent of dissolution or the resulting alkalinity. Once the system is well-mixed, the reaction is limited by other factors such as temperature or concentration, not by how fast it is stirred (Nanda *et al.* 2024). As more RHA is added to the NaOH solution, more silica dissolves. This dissolved silica reacts with the OH^- ions from the sodium hydroxide to form alkali activator. This reaction consumes the free hydroxide ions, thereby lowering the pH and the overall alkalinity of the solution. Essentially, the solution becomes more siliceous and less alkaline (Samuel Owoeye 2017).

Figures 5e and 5f demonstrated that alkalinity decreased as the heating temperature increased when RHA quantity was kept constant. Higher temperatures provide more kinetic energy to the system, which accelerates the endothermic reaction between the amorphous silica in the RHA and the NaOH solution. The chemical reaction that produces sodium silicate involves the consumption of hydroxide ions (OH^-). As the temperature rises, the reaction proceeds more completely, dissolving more silica. Since the reaction

consumes the free sodium hydroxide to form silicate species, the concentration of free OH^- ions (alkalinity) in the final solution decreases (Handayani *et al.* 2022).

Moreover, Figs. 5g and 5h show that alkalinity tended to increase when heating time increased. As the heating duration was extended, more silica was dissolved from the ash into the solution. The extended time ensures that the reaction reaches a higher degree of completion, resulting in a higher concentration of dissolved silicate species and a stable alkaline solution. While alkalinity and silica yield increased with time, research indicated that the most significant gains occurred within the first three hours. Beyond this optimum duration, the increase in dissolution, and thus alkalinity, becomes marginal and may not justify the additional energy consumption (Tong *et al.* 2018).

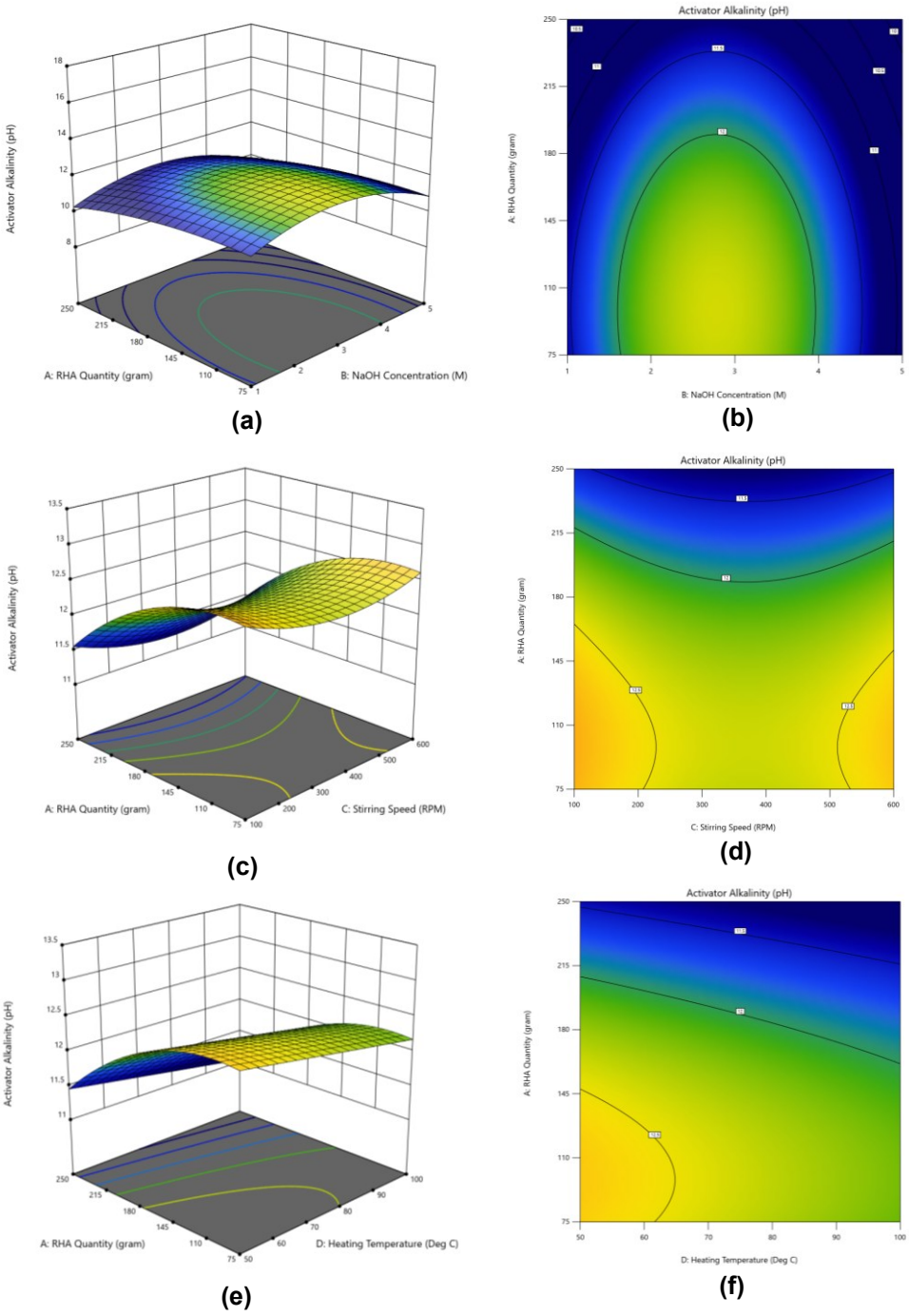

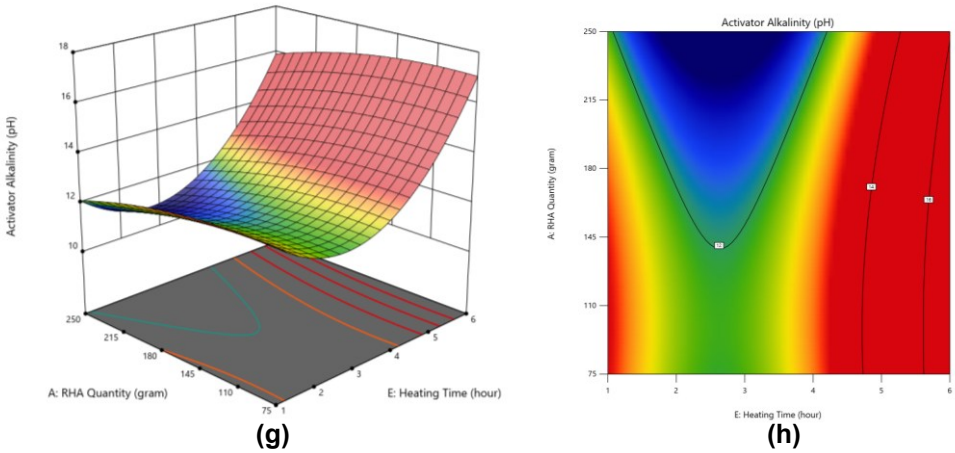

Fig. 5. 3D RSM plots and contour plots of two factors on the activator alkalinity where the other three factors are kept constant

Effect of Variables on Silica Composition

Mathematical model for predicting silica composition of alternative activator

The best-fitting mathematical model from RSM was found to be a reduced quadratic model. A term-reduction procedure using backward elimination was applied to remove statistically insignificant interaction terms ($P > 0.05$). Consequently, no interaction terms were included in the final reduced model to avoid modeling noise and improve predictive accuracy. Equation 3 is a mathematical model based on actual factor terms for predicting silica composition.

$$R2 = +17.1531+0.6317A+0.3883B-0.0025C-0.1183D+6.6034E-0.0002A^2 -0.2157B^2-1.2724E^2 \quad (3)$$

Equation 3 shows that the stirring speed (C) and heating temperature (D) had negative effects on the silica composition, meanwhile the RHA quantity (A), NaOH concentration (B), and heating time (E) had synergistic effects. In addition, the second-order term A^2, B^2, and E^2 posed unfavorable effects.

ANOVA for the predicted quadratic model

Table 4 shows ANOVA results based on the RSM study produced by Stat-Ease 360 version 25.0.6. The P-value for the quadratic model of alternative activator silica composition was significant ($P < 0.0001$), which shows that the results were significant, and the model was excellent for predicting the response (alternative activator silica composition). Furthermore, the model F-value of 55.8058 implies the model was significant since there was only a 0.01% chance that an F-value this large could occur due to noise. In this case, A, B, C, D, E, A^2, B^2, and E^2 were significant model terms (note: A is RHA quantity; B is NaOH concentration; C is stirring speed; D is heating temperature; E is heating time). Therefore, the hypothesis of this study—the significant effect of factors—was confirmed. Values greater than 0.1000 indicate the model terms were not significant. Statistical insignificance indicates that the study lacks sufficient evidence to prove that the variable being tested had any effect. Most importantly, A, B, C, D, E, A^2,

B^2, and E^2 had P-values lower than 0.1000. It means that all those variables were significant in the model.

The R^2 of 0.9159 achieved is indicative that the model produced was valid and closely fitted to the experimental data. This result is similar to one reported by Adamu *et al.* (2019). The predicted R^2 of 0.8850 is in reasonable agreement with the adjusted R^2 of 0.8995. The difference between predicted R^2 and adjusted R^2 was found to be 0.0145, which is within the required limit (not more than 0.2) for a good model. R^2 can be improved by addition of more independent variables; therefore, goodness of fit cannot be concluded from value of R^2 alone. Conversely adjusted R^2 only increases with variables that have strong correlation with the dependent variable otherwise it decreases. On the other hand, predicted R^2 is an indication of how well the model developed produces responses for new observation and whether the model is complicated or not. Therefore, adjusted R^2 and predicted R^2 are more desirable properties for goodness of fit in statistics. In this model, the R^2 value was close to 1. The adequate precision value of 30.8293 shows that it is higher than 4 and, therefore, offers an adequate signal-to-noise ratio. The mean silica composition value of alternative activator was 16.5772. The standard deviation in activator silica composition was ± 0.3571, which is acceptable, while the coefficient of variation (CV %) in activator silica composition was 2.1541%, below the acceptable level of 10%, reflecting a good model. The descriptive statistics of the model, factors' sum of the squares, and mean square values are shown in Table 4.

Table 4. ANOVA for Quadratic Model of Silica Composition

Source	Sum of Squares	Degree of Freedom (df)	Mean Square	F-value	*P*-value	Significance
Model	56.9284	8	7.1161	55.8058	< 0.0001	significant
A-RHA Quantity	2.7862	1	2.7862	21.8501	< 0.0001	
B-NaOH Concentration	5.6786	1	5.6786	44.5325	< 0.0001	
C-Stirring Speed	2.1228	1	2.1228	16.6474	0.0002	
D-Heating Temperature	32.8086	1	32.8086	257.2928	< 0.0001	
E-Heating Time	9.2697	1	9.2697	72.6951	< 0.0001	
A^2	3.3670	1	3.3670	27.5957	< 0.0001	
B^2	1.2301	1	1.2301	9.6464	0.0034	
E^2	8.9148	1	8.9148	69.9120	< 0.0001	
Std. Dev.	0.3571		R^2	0.9159		
Mean	16.5772		Adjusted R^2	0.8995		
CV %	2.1541		Predicted R^2	0.8850		
PRESS	7.1495		Adequate Precision	30.8293		

Diagnostics of actual versus predicted responses

Considering the positive note of the prediction model from the statistics, the Stat-Ease Software gives other diagnostic tools based on the experimental data and model for further analysis. The predicted *versus* actual plot and residual *versus* predicted are discussed here. These graphs help to understand if there are any outliers in the experimental results (Fig. 6). The predicted plot of the actual responses is roughly a straight line, which shows the model's good quality in predicting the responses (Fig. 6a). Since the R^2 value is 0.9159, 92% of the data points were around the fitted regression line, with only 8% of residues. The correlation between the predicted and actual activator silica composition, and the linearity shows the model is useful for predicting the silica composition efficiently. Meanwhile, the residual versus predicted plots (Fig. 6b) show constant variants with no specific trends and no outliers (no points above the red line).

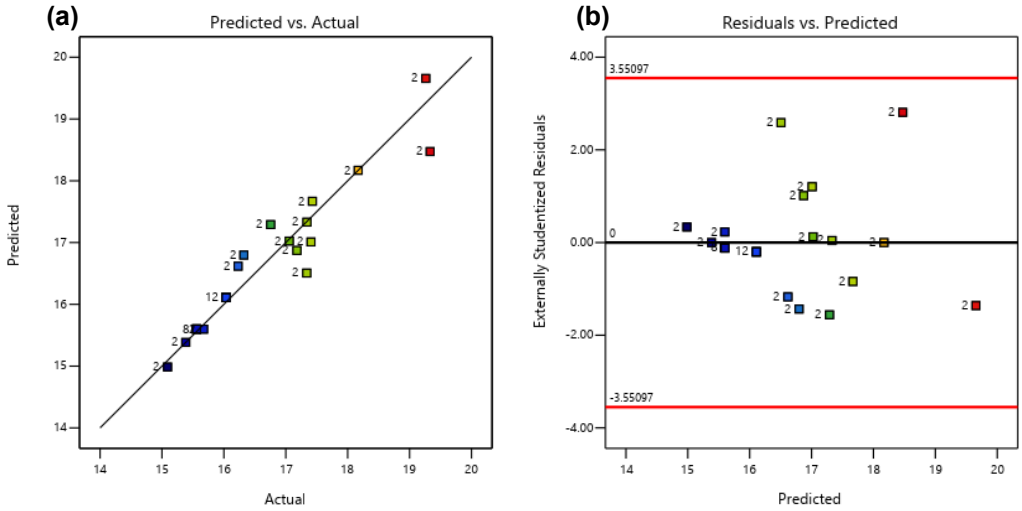

Fig. 6. a: Predicted *vs*. actual plot; and b. Residuals *vs*. predicted

Analysis of response surface plots of silica composition

Figure 7 represents the three-dimensional response plots of the effects of two independent variables at a time on the alternative activator silica composition, while keeping the other variables constant. It reflects the absence of statistically significant interaction terms in the model. Figures 7a and 7b show that the silica composition of the alternative activator tends to reach an optimum as the RHA quantity and NaOH concentration increase. After attaining the optimum peak, the silica composition decreased with increasing RHA quantity and NaOH concentration. Firstly, increasing the RHA quantity and NaOH concentration improves silica composition because the chemical conditions promote the breakdown of the silica network. Higher NaOH concentrations increase the number of hydroxide ions (OH^-). These ions attack the siloxane bonds (Si-O-Si) in the amorphous silica of the RHA, breaking them down into soluble silicates. Increasing the RHA quantity simply provides more source material (silica) to be dissolved, which initially drives up the concentration of dissolved silica in the solution. After reaching the optimum peak, further increases lead to a decrease in the measured silica composition because the response is evaluated as the weight percentage (wt%) of silica within the dried solid residue. When the NaOH concentration exceeds the optimal ratio required for extraction, the excess unreacted NaOH remains in the filtrate. Upon drying, this excess NaOH contributes significantly to the total solid mass, thereby diluting the relative weight

percentage of silica. Similarly, adding RHA beyond the solubility limit of the alkaline solution does not yield more dissolved silica, as the excess undissolved ash is simply removed during filtration (Muñoz-Castillo *et al.* 2025).

Figures 7c and 7d show that the silica composition decreased when the stirring speed increased and RHA quantity constant. Initially, stirring helps dissolve silica by reducing the boundary layer thickness around particles, which aids mass transfer. However, once the stirring speed is high enough to eliminate diffusion resistance, the reaction becomes controlled by the chemical reaction rate itself. Beyond a certain speed, increasing agitation does not significantly speed up the breakage of siloxane bonds (Si-O-Si). Excessively high stirring speeds can disturb the equilibrium or stability of the solution without adding benefit, leading to diminishing returns where the measured soluble silica might slightly decrease due to physical disturbances or precipitation issues (Al-Abboodi *et al.* 2020).

Figures 7e and 7f demonstrated that the silica composition decreased as the heating temperature increased when RHA quantity was kept constant. At temperatures above a certain threshold, the amorphous silica dissolved in the solution can begin to crystallize into less soluble forms, such as low-quartz or cristobalite. This crystallization removes silica from the liquid phase, effectively lowering the measured silica composition in the solution. While higher temperatures generally accelerate initial dissolution initially, excessive heat can lead to rapid saturation and the formation of a localized silica-rich gel layer around unreacted RHA particles, which impedes further extraction (Nzereogu *et al.* 2023). Furthermore, because the silica composition is determined as a weight percentage (wt%) of the dried solid residue using EDX, excessive heating temperatures increase water evaporation during synthesis. This evaporation concentrates the unreacted NaOH in the filtrate. Upon drying, this excess sodium hydroxide contributes a larger mass fraction to the solid residue, thereby diluting the relative weight percentage of the extracted silica (Setyawan *et al.* 2019). In some experimental setups, increasing the temperature beyond the optimum (*e.g.*, 80 °C) provided no significant increase in silica yield. In fact, prolonged heating or excessive temperatures can lead to the formation of stable, insoluble silicate species that do not contribute to the active silica content in the activator (Tong *et al.* 2018).

Moreover, Figs. 7g and 7h show that silica composition of alternative activator tended to reach optimum values as the RHA quantity and heating time increased. Initially, extending the heating duration provided sufficient time for the hydroxide ions to attack the siloxane bonds (Si-O-Si) and extract more amorphous silica from the RHA. Simultaneously, an optimal RHA quantity ensured that enough source material was available to be dissolved. After reaching the optimum point, further increases in RHA and heating time led to a decrease in the measured silica composition. As observed with elevated temperatures, prolonged heating times exacerbated evaporative losses, which concentrated the unreacted NaOH in the solution and ultimately diluted the measured weight percentage of silica in the dried residue (Nanda *et al.* 2024).

Optimization of Alternative Alkali Activator Synthesis

Figure 8 illustrates the numerical optimization results in terms of ramp graphs, which are used to clarify the results. Numerical optimization uses a ramp graph to clarify the results. Generally, depending on the aim of the research, the design factors and responses are set to achieve the study's objective (Abdellatief *et al.* 2023). For this study, the responses, namely, activator alkalinity and silica composition, were set to the maximum option, and factors including RHA quantity, NaOH concentration, stirring speed, heating

temperature, and heating time were set in the range option. Based on Fig. 8, the optimum conditions for maximum responses were RHA quantity of 162.5 g; NaOH concentration of 3M; stirring speed of 350 RPM; heating temperature of 75 °C; and heating time of 3.5 h. In addition, the desirability value was 0.692 for this response. Although moderate, this value indicated that the formulation was sufficiently desirable to fulfil the responses' objectives (Raut *et al.* 2025).

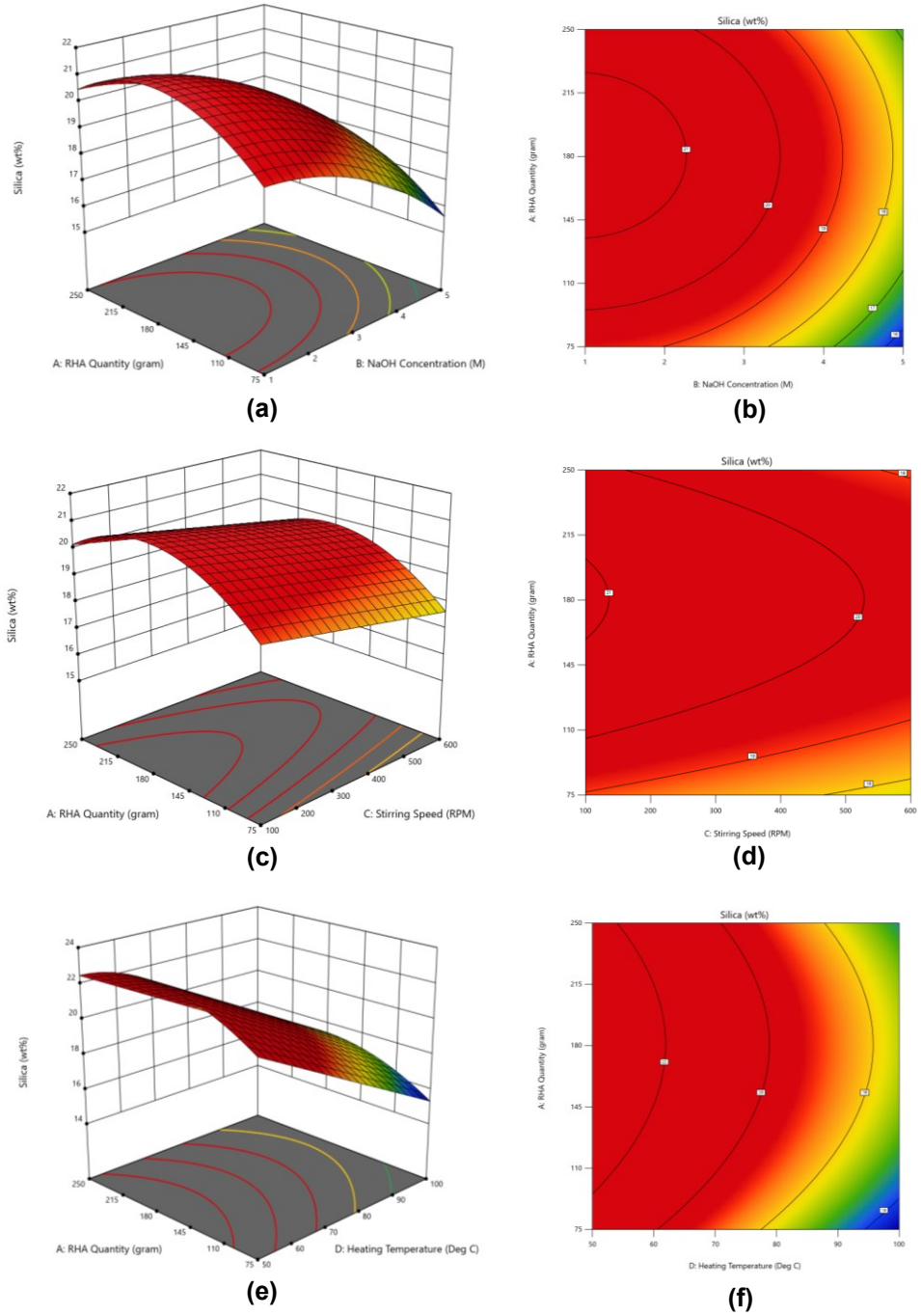

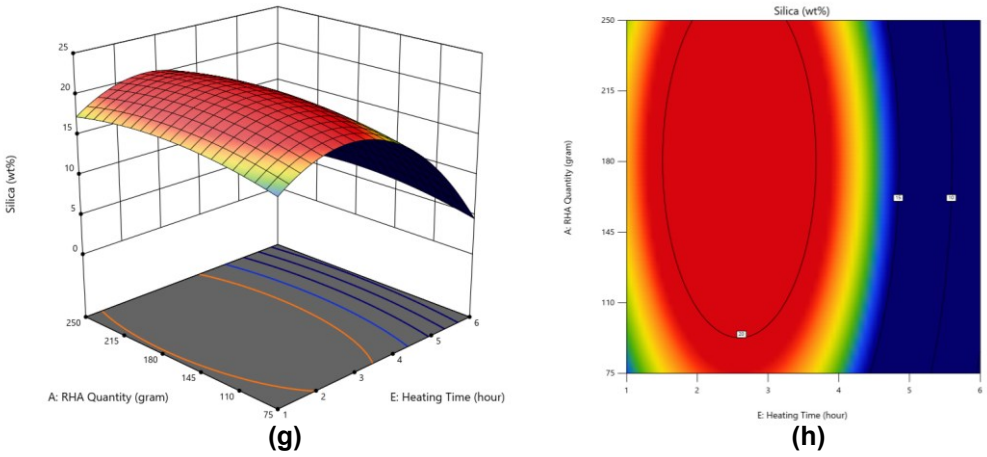

Fig. 7. 3D RSM plots and contour plots of two factors on the silica composition where the other three factors are kept constant

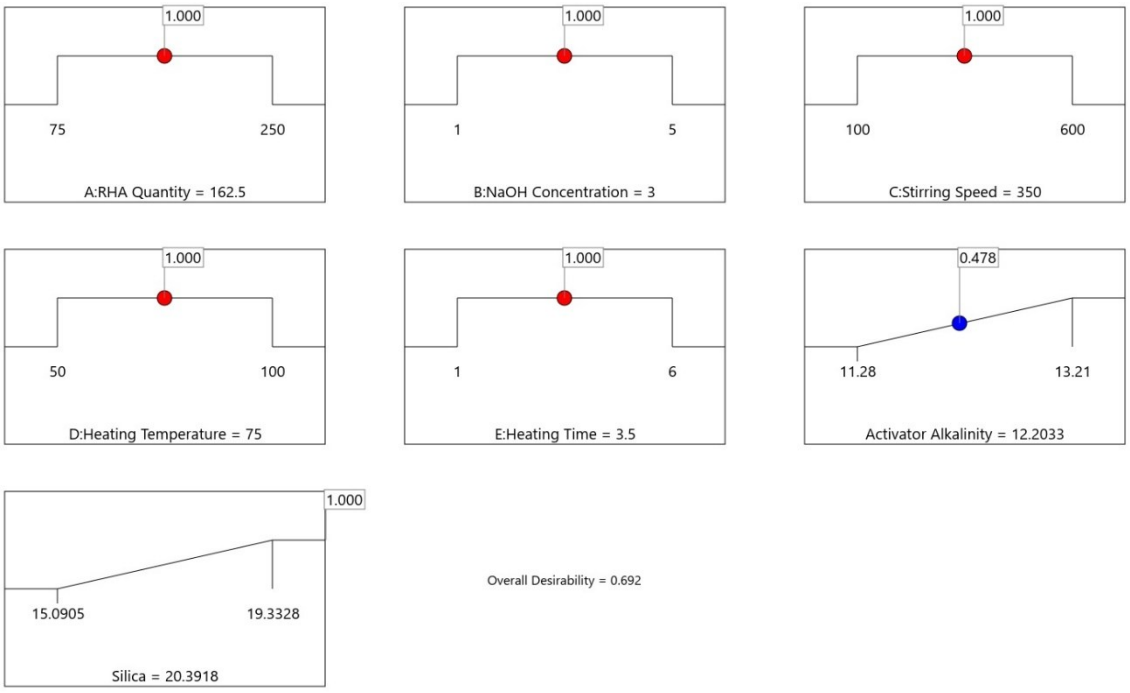

Fig. 8. Ramp chart for statistically optimized factors and response for experimental design

Confirmatory Runs of the Predicted Optimal Response

Statistical literature and practitioners have long advocated the use of confirmation experiments as the final stage of a sequence of designed experiments. The confirmation is to verify that the optimal operating conditions identified as part of an RSM strategy are attainable. Moreover, it is also able to achieve the value of the response desired. Predicted values for confirmation tests were suggested by the Stat-Ease software. For each model, three experiments have been done.

The confirmation location for the confirmatory runs was at RHA quantity of 162.5 g; NaOH concentration of 3M; stirring speed of 350 RPM; heating temperature of 75 °C; and heating time of 3.5 h. The activator alkalinity (pH) for confirmation run 1, 2, and 3

was 12.0; 12.1; and 12.2, respectively. Meanwhile, confirmation experiments 1, 2, and 3 for silica composition (wt%) were 22.6; 25.8; and 12.5, correspondingly. The result of confirmation experiment is summarized in Table 5.

According to the validation criteria of the Stat-Ease software, the reported 95% prediction interval (PI) represents the expected range for the mean of the three confirmatory runs (n=3), rather than the broader interval expected for individual future observations. For activator alkalinity, both the individual runs and the data mean fell well within the 95% PI. For the silica composition, while the individual runs exhibited substantial variability and fell outside this narrow band, the overall data mean (20.3 wt%) successfully fell within the required 95% PI limits (19.6 to 21.2 wt%). Because the prediction interval for an average of multiple runs is mathematically narrower than that for a single run, it is statistically acceptable for individual data points to fall outside the boundaries provided the mean is successfully verified.

Nevertheless, this large dispersion among the individual silica composition runs indicates that while the mathematical model accurately predicts the average trend, the actual silica yield from batch to batch under these optimum conditions may vary considerably due to the complex nature of the extraction and drying procedures. Thus, operating at these settings should reliably produce the targeted alkalinity, but the silica yield should be interpreted as a scientifically validated average expectation rather than a precise batch-by-batch outcome.

Table 5. Summary of Confirmatory Runs

Analysis	Predicted Mean	Predicted Median	Std Dev	n	SE Pred	95% PI Low	Data Mean	95% PI High
Activator Alkalinity	12.2033	12.2033	0.0963	3	0.1058	11.9895	12.0867	12.4171
Silica Composition	20.3918	20.3918	0.3571	3	0.3918	19.6006	20.3105	21.1830

CONCLUSIONS

1. The application of Response Surface Methodology (RSM) with a Central Composite Design (CCD) proved highly effective in modeling the alkali treatment of rice husk ash (RHA). The developed reduced quadratic models accurately predicted the activator alkalinity and silica composition, revealing that RHA quantity, NaOH concentration, heating temperature, and heating time significantly dictate the extraction efficiency, whereas stirring speed showed no significant statistical impact.
2. The optimum conditions for maximizing both alkalinity and silica extraction were identified as an RHA quantity of 162.5 g, NaOH concentration of 3M, stirring speed of 350 RPM, heating temperature of 75 °C, and heating time of 3.5 h. These parameters establish a balanced thermochemical environment that provides sufficient hydroxide ions to break down siloxane bonds without causing excessive evaporation or unwanted silica saturation.
3. Confirmatory runs validated the optimization models, as the data means for both activator alkalinity (12.1) and silica composition (20.3 wt%) successfully fell within their respective 95% Prediction Intervals for the mean. While the alkalinity response

was highly repeatable across individual runs, the silica composition exhibited substantial batch-to-batch variability. This indicates that while the mathematical model accurately predicts the average expected yield, the exact silica composition per batch may fluctuate. Furthermore, while this study successfully demonstrates a pathway to reduce reliance on commercial activators, future research should focus on refining the extraction and filtration controls to minimize this variability and subsequently evaluate the life-cycle and economic feasibility of scaling up this waste-derived activator for industrial geopolymer production.

ACKNOWLEDGMENTS

The authors would like to express the highest gratitude and appreciation to Universiti Malaysia Sarawak (UNIMAS) for providing the opportunity and support to conduct this research. This research is also funded by Princess Nourah bint Abdulrahman University Researchers Supporting Project number (PNURSP2026R24).

Conflict of Interest

The authors declare that there is no conflict of interest regarding the publication of this manuscript.

Use of Generative AI

The authors affirm that there is no generative AI platforms that were used to create, draft, or revise the core scientific content. The conceptualization, data collection, analysis, and interpretation of findings were conducted solely by the researchers.

REFERENCES CITED

Abdellatief, M., Mortagi, M., Elrahman, M. A., Tahwia, A. M., Alluqmani, A. E., and Alanazi, H. (2023). "Characterization and optimization of fresh and hardened properties of ultra-high performance geopolymer concrete," *Case Studies in Construction Materials* 19(April), article e02549. https://doi.org/10.1016/j.cscm.2023.e02549

Adamu, M., Rahman, M. R., and Hamdan, S. (2019). "Formulation optimization and characterization of bamboo/polyvinyl alcohol/clay nanocomposite by response surface methodology," *Composites Part B: Engineering* 176(July), article 107297. https://doi.org/10.1016/j.compositesb.2019.107297

Adesanya, E., Perumal, P., Luukkonen, T., Yliniemi, J., Ohenoja, K., Kinnunen, P., and Illikainen, M. (2021). "Opportunities to improve sustainability of alkali-activated materials: A review of side-stream based activators," *Journal of Cleaner Production* 286, article 125558. https://doi.org/10.1016/j.jclepro.2020.125558

Al-Abboodi, S. M. T., Al-Shaibani, E. J. A., and Alrubai, E. A. (2020). "Preparation and characterization of nano silica prepared by different precipitation methods," *IOP Conference Series: Materials Science and Engineering* 978(1), article 012031. https://doi.org/10.1088/1757-899X/978/1/012031

Al-Alwan, A. A. K., Al-Bazoon, M., I.Mussa, F., Alalwan, H. A., Hatem Shadhar, M., Mohammed, M. M., and Mohammed, M. F. (2024). "The impact of using rice husk

ash as a replacement material in concrete: An experimental study," *Journal of King Saud University - Engineering Sciences* 36(4), 249-255. https://doi.org/10.1016/j.jksues.2022.03.002

Alawadhi, K., Alzuwayer, B., Mohammad, T. A., and Buhemdi, M. H. (2021). "Design and optimization of a centrifugal pump for slurry transport using the response surface method," *Machines* 9(3). https://doi.org/10.3390/machines9030060

Albert Daud, F. A., Ismail, I., Ahmadi, R., and Binti Abdul Samat, N. A. S. (2020). "Characterization of alkali-activated palm oil fuel ash pastes as a function of calcination temperatures of raw precursor," *Materials Performance and Characterization* 9(1), 36-49. https://doi.org/10.1520/MPC20190212

Alkharisi, M. K., and Dahish, H. A. (2025). "The application of response surface methodology and machine learning for predicting the compressive strength of recycled aggregate concrete containing polypropylene fibers and supplementary cementitious materials," *Sustainability* 17(7), article 2913. https://doi.org/10.3390/su17072913

Alnahhal, M. F., Hamdan, A., Hajimohammadi, A., Castel, A., and Kim, T. (2024). "Hydrothermal synthesis of sodium silicate from rice husk ash: Effect of synthesis on silicate structure and transport properties of alkali-activated concrete," *Cement and Concrete Research* 178(September 2023), article 107461. https://doi.org/10.1016/j.cemconres.2024.107461

Alnahhal, M. F., Kim, T., and Hajimohammadi, A. (2021). "Waste-derived activators for alkali-activated materials: A review," *Cement and Concrete Composites*, Elsevier Ltd, 118(February), 103980. https://doi.org/10.1016/j.cemconcomp.2021.103980

Barragán-Ramírez, R., González-Hernández, A., Bautista-Ruiz, J., Ospina, M., and Aperador Chaparro, W. (2024). "Enhancing concrete durability and strength with fly ash, steel slag, and rice husk ash for marine environments," *Materials* 17(12), article 3001. https://doi.org/10.3390/ma17123001

Bezerra, B. P., Morelli, M. R., and Luz, A. P. (2023). "Effect of reactive silica sources on the properties of Na-metakaolin-based geopolymer binder," *Construction and Building Materials* 364(November 2022), article 129989. https://doi.org/10.1016/j.conbuildmat.2022.129989

Chen, H. Y., and Chen, C. (2025). "Importance of using modern regression analysis for response surface models in science and technology," *Applied Sciences* 15(13), 1-38. https://doi.org/10.3390/app15137206

Cong, P., Du, R., Gao, H., and Chen, Z. (2024). "Comparison and assessment of carbon dioxide emissions between alkali-activated materials and OPC cement concrete," *Journal of Traffic and Transportation Engineering (English Edition)*, Periodical Offices of Chang'an University, 11(5), 918-938. https://doi.org/10.1016/j.jtte.2023.07.011

Endale, S. A., Taffese, W. Z., Vo, D. H., and Yehualaw, M. D. (2023). "Rice husk ash in concrete," *Sustainability* 15(1), article 137. https://doi.org/10.3390/su15010137

Farooq, F., Roy, T., Ali, M. H., Ridoy, M. A. R., Kashem, A., Rahman, L., and Das, A. (2026). "Prediction of mechanical strengths of geopolymer concrete using optimized machine learning models with graphical user interface," *Journal of Building Pathology and Rehabilitation* 11(1). https://doi.org/10.1007/s41024-025-00704-7

Font, A., Soriano, L., de Moraes Pinheiro, S. M., Tashima, M. M., Monzó, J., Borrachero, M. V., and Payá, J. (2020). "Design and properties of 100% waste-based ternary alkali-activated mortars: Blast furnace slag, olive-stone biomass ash and rice husk

ash," *Journal of Cleaner Production* 243, article 118568. https://doi.org/10.1016/j.jclepro.2019.118568

Gao, B., Jang, S., Son, H., Park, S., Lee, H. S., and Bae, C. J. (2022). "Phase transformation and microstructure evolution of a kaolin-based precursor," *Ceramics International* 48(24), 36066-36075. https://doi.org/10.1016/j.ceramint.2022.08.035

Ghelich, R., Jahannama, M. R., Abdizadeh, H., Torknik, F. S., and Vaezi, M. R. (2019). "Central composite design (CCD) – Response surface methodology (RSM) of effective electrospinning parameters on PVP-B-Hf hybrid nanofibrous composites for synthesis of HfB 2 -based composite nanofibers," *Composites Part B: Engineering* 166(August 2018), 527-541. https://doi.org/10.1016/j.compositesb.2019.01.094

Girish, M. G., Prashant, S., Jagadisha, H. M., and Prabha, S. (2026). "Development of one part sustainable alkali activated binder system using slag, flyash and micro calcined kaolin," *Scientific Reports* 16(1), 1-20. https://doi.org/10.1038/s41598-026-46876-1

Hamidu, I., Afotey, B., Kwakye-Awuah, B., and Anang, D. A. (2025). "Synthesis of silica and silicon from rice husk feedstock: A review," *Heliyon* 11(4), article e42491. https://doi.org/10.1016/j.heliyon.2025.e42491

Handayani, L., Aprilia, S., Abdullah, Rahmawati, C., Aulia, T. B., Ludvig, P., and Ahmad, J. (2022). "Sodium silicate from rice husk ash and their effects as geopolymer cement," *Polymers* 14(14), article 2920. https://doi.org/10.3390/polym14142920

He, J., Jie, Y., Zhang, J., Yu, Y., and Zhang, G. (2013). "Synthesis and characterization of red mud and rice husk ash-based geopolymer composites," *Cement and Concrete Composites* 37(1), 108-118. https://doi.org/10.1016/j.cemconcomp.2012.11.010

Kallamalayil Nassar, A., and Kathirvel, P. (2023). "Effective utilization of agricultural waste in synthesizing activator for sustainable geopolymer technology," *Construction and Building Materials* 362(October 2022), article 129681. https://doi.org/10.1016/j.conbuildmat.2022.129681

Kamseu, E., Beleuk à Moungam, L. M., Cannio, M., Billong, N., Chaysuwan, D., Melo, U. C., and Leonelli, C. (2017). "Substitution of sodium silicate with rice husk ash-NaOH solution in metakaolin based geopolymer cement concerning reduction in global warming," *Journal of Cleaner Production* 142, 3050-3060. https://doi.org/10.1016/j.jclepro.2016.10.164

Khalid, A. A., Gora, A. M., Rafindadi, A. D., Haruna, S. I., and Ibrahim, Y. E. (2024). "Response surface methodology approach for the prediction and optimization of the mechanical properties of sustainable laterized concrete incorporating eco-friendly calcium carbide waste," *Infrastructures* 9(11), article 206. https://doi.org/10.3390/infrastructures9110206

Kim, J., Fumino, H., and Kanematsu, M. (2025). "Effects of rice husk ash particle size and luxan value influence on mortar properties and proposal of hydration ratio measurement method," *Materials* 18(1), article 21. https://doi.org/10.3390/ma18010021

Kordi, M., Farrokhi, N., Pech-Canul, M. I., and Ahmadikhah, A. (2024). "Rice husk at a glance: From agro-industrial to modern applications," *Rice Science* 31(1), 14-32. https://doi.org/10.1016/j.rsci.2023.08.005

Luukkonen, T., Abdollahnejad, Z., Yliniemi, J., Kinnunen, P., and Illikainen, M. (2018). "Comparison of alkali and silica sources in one-part alkali-activated blast furnace

slag mortar," *Journal of Cleaner Production* 187, 171-179. https://doi.org/10.1016/j.jclepro.2018.03.202

Maaze, M. R., Das, S. K., Garg, N., and Shrivastava, S. (2025). "Economic-environmental and multi-criteria optimization for predicting alkaline ratios in waste cement concrete-based geopolymer using central composite design," *International Journal of Concrete Structures and Materials* 19(1), article 35. https://doi.org/10.1186/s40069-025-00767-3

Muñoz-Castillo, A., Sánchez-Soto, P. J., and Eliche-Quesada, D. (2025). "Valorisation of rice husk ash as an activator in the preparation of alkali-activated cements based on electric arc furnace slag," *Archives of Civil and Mechanical Engineering* 25(3), 1-26. https://doi.org/10.1007/s43452-025-01209-3

Nair, D. G., Fraaij, A., Klaassen, A. A. K., and Kentgens, A. P. M. (2008). "A structural investigation relating to the pozzolanic activity of rice husk ashes," *Cement and Concrete Research* 38(6), 861-869. https://doi.org/10.1016/j.cemconres.2007.10.004

Nanda, B., Mishra, J., and Patro, S. K. (2024). "Synthesis of rice husk ash based alkaline activators for geopolymer binder systems: A review," *Journal of Building Engineering* 91(May), article 109694. https://doi.org/10.1016/j.jobe.2024.109694

Neupane, K. (2022). "Evaluation of environmental sustainability of one-part geopolymer binder concrete," *Cleaner Materials* 6(2), article 100138. https://doi.org/10.1016/j.clema.2022.100138

Niu, Y., Hu, W., Shen, T., Dong, K., and Wang, D. (2022). "Response surface methodology for the optimization of Zn-contaminated soil remediation by soil washing with water-soluble chitosan," *ACS Omega* 7(46), 41929-41936. https://doi.org/10.1021/acsomega.2c03181

Nzereogu, P. U., Omah, A. D., Ezema, F. I., Iwuoha, E. I., and Nwanya, A. C. (2023). "Silica extraction from rice husk: Comprehensive review and applications," *Hybrid Advances* 4(August), article 100111. https://doi.org/10.1016/j.hybadv.2023.100111

Pattanayak, N., Behera, H. K., and Das, S. S. (2024). "Mix design strategy and optimization considering characteristic evaluation of geopolymer concrete," *Journal of Building Engineering* 91(February), article 109557. https://doi.org/10.1016/j.jobe.2024.109557

Rajan, H. S., and Kathirvel, P. (2021). "Sustainable development of geopolymer binder using sodium silicate synthesized from agricultural waste," *Journal of Cleaner Production* 286, article 124959. https://doi.org/10.1016/j.jclepro.2020.124959

Raut, A., Adamu, M., Janga, S., Maaze, M. R., Ibrahim, Y. E., and Alanazi, H. (2025). "Optimizing glass powder and slag-based geopolymers: enhancing thermo-mechanical strength resistance for sustainable construction applications," *Ain Shams Engineering Journal* 16(8), article 103477. https://doi.org/10.1016/j.asej.2025.103477

Ricciotti, L., Lucariello, D., Perrotta, V., Apicella, A., and Aversa, R. (2025). "Sustainable alkali-activated and geopolymer materials: What is the future for Italy?," *Recycling* 10(4), 140. https://doi.org/10.3390/recycling10040140

Rocha, S., Ascensão, G., and Maia, L. (2023). "Exploring design optimization of self-compacting mortars with response surface methodology," *Applied Sciences* 13(18), article 10428. https://doi.org/10.3390/app131810428

Samuel Owoeye, S. (2017). "Effects of extraction temperature and time on the physical properties of soluble sodium silicate from rice husk ash," *Science Journal of Chemistry* 5(1), 8. https://doi.org/10.11648/j.sjc.20170501.12

Sarma, J., Rajkhowa, S., and Das, S. (2024). "Synthesis of white silica from 'Joha Rice Husk' (a special rice variety of Assam, India), characterization and determination of its point of zero charge (pHPZC)," *Journal of Chemistry* 2024(1), article 5542855. https://doi.org/10.1155/joch/5542855

Setyawan, N., Hoerudin, and Wulanawati, A. (2019). "Simple extraction of silica nanoparticles from rice husk using technical grade solvent: Effect of volume and concentration," *IOP Conference Series: Earth and Environmental Science* 309(1), article 012032. https://doi.org/10.1088/1755-1315/309/1/012032

Sompech, S., Dasri, T., and Thaomola, S. (2016). "Preparation and characterization of amorphous silica and calcium oxide from agricultural wastes," *Oriental Journal of Chemistry* 32(4), 1923-1928. https://doi.org/10.13005/ojc/320418

Tchakouté, H. K., Rüscher, C. H., Kong, S., and Ranjbar, N. (2016). "Synthesis of sodium waterglass from white rice husk ash as an activator to produce metakaolin-based geopolymer cements," *Journal of Building Engineering* 6, 252=261. https://doi.org/10.1016/j.jobe.2016.04.007

Tong, K. T., Vinai, R., and Soutsos, M. N. (2018). "Use of Vietnamese rice husk ash for the production of sodium silicate as the activator for alkali-activated binders," *Journal of Cleaner Production* 201, 272-286. https://doi.org/10.1016/j.jclepro.2018.08.025

Trevizan Pelissaro, D., Bruschi, G. J., Pavan Korf, E., and Dalla Rosa, F. (2023). "Rice husk ash as an alternative soluble silica source for alkali-activated metakaolin systems applied to recycled asphalt pavement stabilization," *Transportation Geotechnics* 39(January), article 100940. https://doi.org/10.1016/j.trgeo.2023.100940

Veza, I., Spraggon, M., Fattah, I. M. R., and Idris, M. (2023). "Response surface methodology (RSM) for optimizing engine performance and emissions fueled with biofuel: Review of RSM for sustainability energy transition," *Results in Engineering* 18(May), article 101213. https://doi.org/10.1016/j.rineng.2023.101213

Wan, X., Ren, L., Lv, T., Wang, D., and Wang, B. (2025). "Research on alkali-activated systems based on solid waste-derived activators: A review," *Sustainability* 17(1), article 254. https://doi.org/10.3390/su17010254

Yao, Z., Luo, L., Qin, Y., Cheng, J., and Qu, C. (2024). "Research on mix design and mechanical performances of MK-GGBFS based geopolymer pastes using central composite design method," *Scientific Reports* 14(1), 1-15. https://doi.org/10.1038/s41598-024-59872-0

Zulfiqar, U., Subhani, T., and Wilayat Husain, S. (2015). "Towards tunable size of silica particles from rice husk," *Journal of Non-Crystalline Solids*, 429, 61-69. https://doi.org/10.1016/j.jnoncrysol.2015.08.037

Article submitted: February 9, 2026; Peer review completed: April 14, 2026; Revisions accepted: June 18, 2025; Published: June 26, 2026.
DOI: 10.15376/biores.21.3.7516-7540